Linear stability analysis of parallel shear flows for an inviscid generalized two-dimensional fluid system

Iwayama, Takahiro
Sueyoshi, Masakazu
Watanabe, Takeshi

(Citation)
Journal of Physics A: Mathematical and Theoretical,46(6):065501-065501

(Issue Date)
2013-01

(Resource Type)
journal article

(Version)
Accepted Manuscript

(URL)
https://hdl.handle.net/20.500.14094/90002602

Linear stability analysis of parallel shear flows for an inviscid generalized two-dimensional fluid system

T. Iwayama[1], M. Sueyoshi and T. Watanabe[2]

[1]Department of Earth and Planetary Sciences, Graduate School of Science, Kobe University, Kobe 657-8501, Japan

[2]Department of Scientific and Engineering Simulation, Graduate School of Engineering, Nagoya Institute of Technology, Gokiso, Showa-ku, Nagoya 466-8555, Japan

E-mail: [1]iwayama@kobe-u.ac.jp

Abstract. The linear stability of parallel shear flows for an inviscid generalized two-dimensional (2D) fluid system, the so-called α turbulence system, is studied. This system is characterized by the relation $q = -(-\Delta)^{\alpha/2}\psi$ between the advected scalar q and the stream function ψ. Here, α is a real number not to exceed 3 and q is referred to as the generalized vorticity. In this study, a sufficient condition for linear stability of parallel shear flows is derived using the conservation of wave activity. A stability analysis is then performed for a sheet vortex that violates the stability condition. The instability of a sheet vortex in the 2D Euler system ($\alpha = 2$) is referred to as a Kelvin–Helmholtz (KH) instability; such an instability for the generalized 2D fluid system is investigated for $0 < \alpha < 3$. The sheet vortex is unstable in the sense that a sinusoidal perturbation applied to it grows exponentially with time. The growth rate is finite and depends on the wavenumber of the perturbation as $k^{3-\alpha}$ for $1 < \alpha < 3$, where k is the wavenumber of the perturbation. In contrast, for $0 < \alpha \leq 1$, the growth rate is infinite. In other words, a transition of the growth rate of the perturbation occurs at $\alpha = 1$. A physical model for KH instability in the generalized 2D fluid system, which can explain the transition of the growth rate of the perturbation at $\alpha = 1$, is proposed.

PACS numbers: 47.15.chi, 47.20.Cq, 47.20.Ft, 47.27.Ak, 47.32.ck, 47.32.cb

Submitted to: *J. Phys. A: Math. Gen.*

1. Introduction

Two-dimensional (2D) fluid motions have been actively studied in geophysical fluid dynamics, because large-scale atmospheric and oceanic fluid motions are approximately two-dimensional. A generalized 2D fluid system (the so-called α turbulence system) was proposed as a family of models of 2D geophysical fluids [1]. The governing equations for the generalized 2D fluid system are

$$\frac{\partial q}{\partial t} + J(\psi, q) = \mathcal{D} + \mathcal{F}, \tag{1a}$$

$$-(-\Delta)^{\alpha/2}\psi = q, \tag{1b}$$

where $\psi(\boldsymbol{r},t)$ is the stream function, $q(\boldsymbol{r},t)$ is a scalar field advected by the velocity field $\boldsymbol{v}=\boldsymbol{e}_z\times\boldsymbol{\nabla}\psi$, $\boldsymbol{e}_z$ is a unit vector normal to the plane of motion, J is the 2D Jacobian, α is a real number, Δ is the Laplacian in 2D space, and $\mathcal{D}$ and $\mathcal{F}$ are dissipation and forcing terms, respectively.

Equation (1b) characterizes this system. For $\alpha=2$, q is the vorticity and (1) is the vorticity equation for a 2D incompressible barotropic fluid [the so-called 2D Navier–Stokes (NS) system for $\mathcal{D}=\nu\Delta q$, where ν is the kinetic viscosity, and the 2D Euler system for $\mathcal{D}=0$]. Equation (1) for $\alpha=1$ is the surface quasi-geostrophic (SQG) equation [2, 3], which describes a quasi-geostrophic flow with zero potential vorticity. In this case, q is the temperature field on a flat lower boundary. The SQG equation has been used to investigate the dynamics of circulations on the tropopause [4] and the upper ocean [5]. For $\alpha=-2$, (1) is the Charney-Hasegawa-Mima equation in the asymptotic model regime [6–12], which describes nearly geostrophic motion on scales larger than the deformation radius. We refer to q as the generalized vorticity or simply the vorticity, although it has units $[q]=L^{2-\alpha}T^{-1}$, where L and T are units of length and time, respectively.

The purpose of investigating the generalized 2D fluid system is generally twofold. The first objective is to understand geophysical 2D fluid systems from a unified perspective. The second is to elucidate the universality and peculiarity of prevailing theories for the 2D Euler and NS systems and further develop them.

This system has been actively studied over the past 10 years [13–21]. However, previous work on this system has been devoted to its turbulent properties. Other fundamental topics, such as the stability of parallel shear flows, have not yet been studied. Even a sufficient condition for the linear stability of parallel shear flows has not been known yet. We thus study the linear stability of parallel shear flows for the inviscid generalized 2D fluid system.

The Rayleigh inflection point criterion [22] is a sufficient condition for stability, or necessary condition for instability, for parallel shear flows in the 2D Euler system ($\alpha=2$). This criterion is expressed in terms of vorticity as *"a necessary condition for instability is that the gradient of basic state vorticity,* $\mathrm{d}Q/\mathrm{d}y$*, changes sign somewhere in the flow domain"*. Once we find that the basic state of the flow under consideration violates a sufficient condition for stability, we next examine the stability of such flow by the normal mode analysis. In this sense, the sufficient condition of stability is crucial to the study of the stability of parallel shear flows. Hence, as the first step of this study, a sufficient condition for linear stability is derived. Here, we focus on how Rayleigh's criterion can be generalized to the case of $\alpha\neq2$. It will be shown that this criterion is valid not only for $\alpha=2$, but also for $\alpha\neq2$, if we interpret the vorticity gradient as the generalized vorticity gradient. We shall call this criterion as the generalized Rayleigh's criterion for stability in this paper.

As the next step, we theoretically investigate the linear stability of a sheet vortex, whose generalized vorticity distribution is given by $Q(y)=\delta(y)$. Here $\delta(y)$ is the Dirac delta function. This generalized vorticity profile violates the generalized Rayleigh's

criterion for stability. Therefore we perform normal mode analysis of the sheet vortex. In particular, we focus our attention on the dependence of the growth rate and the spatial structures of perturbations to the basic state on the parameter α. Note that the instability of this vorticity distribution for the 2D Euler system is well known as the Kelvin–Helmholtz (KH) instability problem. We thus examine a KH instability problem for the generalized 2D fluid system in this paper.

To solve the KH instability problem using (1), the jump or matching conditions of the sheet vortex at $y = 0$ are required to match the solutions in the region $y \gtrless 0$. For the 2D Euler system, these conditions are the continuity of pressure and that of the material interface on the sheet vortex. The latter condition is also valid for the generalized 2D fluid system. However, the validity of the former condition is not guaranteed for $\alpha \neq 2$. Therefore, the conventional method of solving the KH instability for the 2D Euler system cannot be applied to the present system. To avoid this difficulty, we introduce a point vortex model for the generalized 2D fluid system and use it to analyze the instability of the sheet vortex. More precisely, we solve the linear instability of an infinite row of equidistant point vortices of equal strength, and take the limit of the distance between the point vortices to zero. The velocity induced by the point vortex is required to formulate the instability of the row of vortices. Fortunately, a Green's function, which is the stream function generated by a point vortex, and the velocity induced by the point vortex, have already been derived by Iwayama and Watanabe [20]. We thus adopt the above mentioned strategy for the linear stability analysis of the sheet vortex.

Here we note that a real parameter α in $(1b)$ does not exceed 3. As discussed by two of the present authors [20], the case $\alpha > 3$ is physically incongruous in the sense that the azimuthal velocity around a velocity source for $\alpha > 3$ is a monotonically increasing function of the distance from the source.

This paper is organized as follows. In section 2, we discuss a sufficient condition for the stability of parallel shear flows for the inviscid generalized 2D fluid system. In section 3, we introduce a point vortex model for the generalized 2D fluid system and perform a linear stability analysis for an infinite row of equidistant point vortices of equal strength. In section 4, we discuss the linear stability of a sheet vortex for the generalized 2D fluid system by taking the limit of the distance between the point vortices to zero. The spatial structures of the perturbation stream function and the perturbation velocity are examined according to a model of the physical instability mechanism of the sheet vortex in section 5. We show that our results demonstrate the validity of the physical mechanism for sheet vortex instability. We summarize the results in section 6.

2. Criterion for stability of parallel shear flows

In this section, the flow domain Ω under consideration is doubly periodic in both directions, periodic in the x-direction and closed in the y-direction (i.e., a zonal channel), or infinite. In the case of a zonal channel ($0 < y < D$), no flows penetrate the boundary. If the domain is infinite, we assume appropriate decay conditions at infinity.

For the 2D Euler system, Rayleigh's criterion can be derived in two ways. The first involves an integral constraint on Rayleigh's equation. The second uses a wave activity conservation law (*e.g.*, [23]). The former derivation requires normal-mode perturbations, but the latter derivation, which we adopt in this study, does not. By introducing a wave activity for the generalized 2D fluid system and proving conservation of wave activity, we derive a sufficient condition for stability in the present system.

We decompose the flow into a basic state consisting of a parallel shear flow and a perturbation indicated by a prime:

$$\psi = \mathfrak{Y}(y) + \psi'(\boldsymbol{r}, t), \tag{2}$$

$$q = Q(y) + q'(\boldsymbol{r}, t), \tag{3}$$

$$\boldsymbol{v} = U(y)\boldsymbol{e}_x + \boldsymbol{v}'(\boldsymbol{r}, t). \tag{4}$$

Here, $\boldsymbol{e}_x$ is the unit vector in the x-direction. We assume that the perturbations are small and that the basic state generalized vorticity gradient $Q_y(\equiv \mathrm{d}Q/\mathrm{d}y)$ is definite sign. Linearizing $(1a)$ with $\mathcal{D} = \mathcal{F} = 0$ about the basic state gives

$$\frac{\partial q'}{\partial t} + U\frac{\partial q'}{\partial x} + Q_y\frac{\partial \psi'}{\partial x} = 0. \tag{5}$$

Multiplying by q', dividing by Q_y, and integrating over the flow domain Ω, we obtain

$$\frac{\mathrm{d}}{\mathrm{d}t}\int_\Omega \frac{1}{2}\frac{{q'}^2}{Q_y}\mathrm{d}\boldsymbol{r} = -\int_\Omega \frac{\partial \psi'}{\partial x}q'\mathrm{d}\boldsymbol{r}. \tag{6}$$

The integrand of the left-hand side of (6), ${q'}^2/(2Q_y)$, is an example of a wave activity density. Its integral is a wave activity. Here, we focus on the right-hand side of (6). Using the Fourier components of ψ' and q' and $(1b)$, we have

$$\int_\Omega \frac{\partial \psi'}{\partial x}q'\mathrm{d}\boldsymbol{r} = \int_\Omega \psi'\frac{\partial q'}{\partial x}\mathrm{d}\boldsymbol{r}. \tag{7}$$

A detailed derivation of (7) is presented in Appendix A. From (7), we obtain

$$\int_\Omega \frac{\partial \psi'}{\partial x}q'\mathrm{d}\boldsymbol{r} = \frac{1}{2}\int_\Omega \frac{\partial}{\partial x}\left(\psi' q'\right)\mathrm{d}\boldsymbol{r} = 0. \tag{8}$$

Substituting (8) into (6), we derive a wave activity conservation law for the generalized 2D fluid:

$$\frac{\mathrm{d}}{\mathrm{d}t}\int_\Omega \frac{1}{2}\frac{{q'}^2}{Q_y}\mathrm{d}\boldsymbol{r} = 0. \tag{9}$$

We note in passing that the integrand of the right-hand side of (6) can be written

$$q'\frac{\partial \psi'}{\partial x} = \boldsymbol{\nabla}\cdot\boldsymbol{F}, \tag{10}$$

$$\boldsymbol{F} = \left(\frac{1}{2}\left[\left(\frac{\partial \psi'}{\partial x}\right)^2 - \left(\frac{\partial \psi'}{\partial y}\right)^2\right], \frac{\partial \psi'}{\partial y}\frac{\partial \psi'}{\partial x}\right) \tag{11}$$

for $\alpha = 2$. In other words, it can be expressed by the divergence of a vector. However, for $\alpha \neq 2$, $q'\partial_x\psi'$ has not been written as the divergence of a vector, and thus wave activity conservation law has not been derived. As shown above, the integral of $q'\partial_x\psi'$ in (8)

can be written as the integral of the divergence of a vector to derive the wave activity conservation law (9). Therefore, the required condition for wave activity conservation is not that $q'\partial_x\psi'$ is the divergence of a vector at every point (for example, (10)), but that the integral of $q'\partial_x\psi'$ over the domain is the integral of the divergence of a vector over the domain.

Using (9), we derive a sufficient condition for stability (*e.g.*, [23]): if Q_y does not change sign in the domain, the perturbation cannot grow. Equivalently, if the perturbation grows, Q_y must change sign somewhere in the domain (a necessary condition for instability). In the case $\alpha = 2$ where $Q = -U_y$, the above condition reduces to Rayleigh's inflection point criterion. Thus, the derived criterion is a generalization of Rayleigh's criterion for the 2D Euler system to the generalized 2D fluid system.

3. Linear stability of point vortex street

In the following sections, we will discuss the stability of an inviscid parallel shear flow that violates the stability criterion derived in the previous section. The simplest and most physically fundamental instance of such flows is presumably a sheet vortex, which is defined by a generalized vorticity distribution of the form $Q(y) = \delta(y)$. Note that the derivation of the Dirac delta function cannot be defined in the ordinally sense. However, it is known that the Dirac delta function can be defined by the limit of some positive definite functions, *e.g.*

$$f_\varepsilon(y) \equiv \frac{\varepsilon}{\pi(y^2+\varepsilon^2)} \tag{12}$$

or

$$g_\varepsilon(y) \equiv \frac{1}{\varepsilon\sqrt{\pi}}\mathrm{e}^{-y^2/\varepsilon^2} \tag{13}$$

as $\varepsilon \to 0$. Since the derivations of the above functions with respect to y are not sign definite, the generalized vorticity distribution $Q(y) = \delta(y)$ can be interpretted as the basic state which violates the generalized Rayleigh's criterion for stability. Thus, it is worth examinig the stability of the sheet vortex concretly. Before discussing the stability of the sheet vortex, we introduce a point vortex model for the present system and investigate the linear stability of an infinite row of equidistant point vortices of equal strength, because the conventional method of solving the KH instability for the 2D Euler equation cannot be applied to the present system as stated in section 1. By taking the limit of the distance between the vortices to zero, we will examine the stability of the sheet vortex for the generalized 2D fluid system in the next section.

3.1. Point vortex model

In this and the following sections, we consider fluid motion on an infinite plane. We introduce a point vortex representation of the form

$$q(\boldsymbol{r},\, t) = \sum_{m=1}^{\infty} \sigma_m \delta(\boldsymbol{r} - \boldsymbol{r}_m(t)), \tag{14}$$

where σ_m is the strength of the point vortex located at the position $\boldsymbol{r}_m$. In particular, we consider the case of $0 < \alpha \leq 3$. Using Green's function for the generalized 2D fluid system [20], the stream function at the position of the vortex is

$$\psi(x_n, y_n) = \begin{cases} \Psi(\alpha) \displaystyle\sum_{\substack{m=1 \\ (m\neq n)}}^{\infty} \frac{\sigma_m}{{r_{nm}}^{2-\alpha}}, & (\alpha \neq 2) \\ \dfrac{1}{2\pi} \displaystyle\sum_{\substack{m=1 \\ (m\neq n)}}^{\infty} \sigma_m \ln r_{nm}, & (\alpha = 2) \end{cases} \tag{15}$$

$$r_{nm} = \sqrt{(x_n - x_m)^2 + (y_n - y_m)^2}, \tag{16}$$

where n is a natural number and $\Psi(\alpha)$ is expressed in terms of the gamma function as

$$\Psi(\alpha) = \begin{cases} -\dfrac{1}{2^\alpha \pi} \dfrac{\Gamma\left(\frac{2-\alpha}{2}\right)}{\Gamma\left(\frac{\alpha}{2}\right)}, & (0 < \alpha < 2) \\ -\dfrac{1}{2^\alpha \left(\Gamma\left(\frac{\alpha}{2}\right)\right)^2 \sin\frac{\alpha\pi}{2}}, & (2 < \alpha) \end{cases} \tag{17}$$

The x- and y-components of velocity of the vortex at $(x_n,\, y_n)$ are

$$\begin{aligned} u(x_n, y_n) &= -\frac{\partial \psi(x_n,\, y_n)}{\partial y_n} \\ &= -(\alpha - 2)\Psi(\alpha) \sum_{\substack{m=1 \\ (m\neq n)}}^{\infty} \frac{\sigma_m (y_n - y_m)}{{r_{nm}}^{4-\alpha}}, \end{aligned} \tag{18}$$

$$\begin{aligned} v(x_n, y_n) &= \frac{\partial \psi(x_n,\, y_n)}{\partial x_n} \\ &= (\alpha - 2)\Psi(\alpha) \sum_{\substack{m=1 \\ (m\neq n)}}^{\infty} \frac{\sigma_m (x_n - x_m)}{{r_{nm}}^{4-\alpha}}, \end{aligned} \tag{19}$$

respectively. The equations of motion for the point vortices are

$$\frac{\mathrm{d}x_n}{\mathrm{d}t} = u(x_n, y_n), \tag{20}$$

$$\frac{\mathrm{d}y_n}{\mathrm{d}t} = v(x_n, y_n). \tag{21}$$

Note that the coefficient that appears in (18) and (19), $(\alpha - 2)\Psi(\alpha)$, is positive definite for the interval $0 < \alpha \leq 3$. It can be rewritten as

$$(\alpha - 2)\Psi(\alpha) = \frac{1}{2^{\alpha-1}\pi} \frac{\Gamma\left(\frac{2-\alpha}{2} + 1\right)}{\Gamma\left(\frac{\alpha}{2}\right)} \tag{22}$$

for the interval $0 < \alpha \leq 2$. Equation (22) indicates that the coefficient is nonzero even at $\alpha = 2$, and takes the value $1/2\pi$ at $\alpha = 2$. Figure 1 shows a plot of $(\alpha - 2)\Psi(\alpha)$ over the interval $0 \leq \alpha \leq 3$. This quantity is exactly equal to $1/2\pi$ at $\alpha = 1$, 2, 3 and is not merely a monotonic increasing function of α. Numerical values of the gamma function are computed using the gammln subroutine in Press *et al* [24].

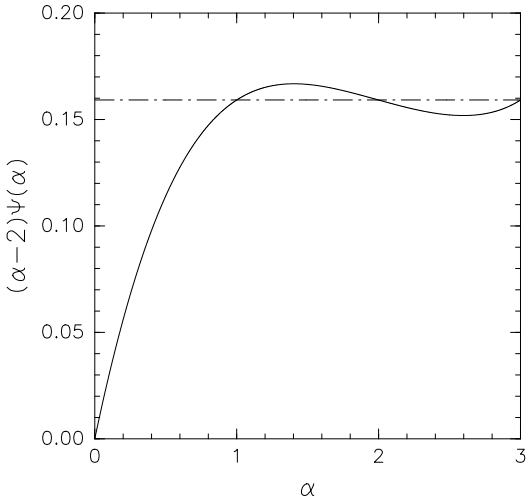

Figure 1. Dependence of $(\alpha-2)\Psi(\alpha)$ on α. The dash-dot line indicates the reference line with the value of $1/2\pi$.

3.2. Linear stability analysis of row of point vortices

We suppose an infinite row of equidistant point vortices of equal strength σ, whose initial coordinates are $(x_n,\, y_n) = (na,\, 0)$, where n is an integer (see figure 2). We discuss the evolution of a perturbation applied to the position of the vortices, $(\delta x_n,\, \delta y_n)$. Given the symmetry of the vortex arrangement, we can concentrate on the vortex motion at the coordinate origin without loss of generality. Therefore, we consider the evolution of a perturbation applied to the vortex at $n = 0$. From equations (18) – (21), and neglecting nonlinear terms for the perturbations, we derive the linearized evolution equations for the perturbations δx_0 and δy_0 as

$$\frac{\mathrm{d}}{\mathrm{d}t}\delta x_0 = -\frac{\sigma}{a^{4-\alpha}}(\alpha-2)\Psi(\alpha)\sum_{m=-\infty}^{\infty}{}' \frac{\delta y_0 - \delta y_m}{|m|^{4-\alpha}}, \tag{23}$$

$$\frac{\mathrm{d}}{\mathrm{d}t}\delta y_0 = -\frac{\sigma}{a^{4-\alpha}}(3-\alpha)(\alpha-2)\Psi(\alpha)\sum_{m=-\infty}^{\infty}{}' \frac{\delta x_0 - \delta x_m}{|m|^{4-\alpha}}, \tag{24}$$

for $\alpha < 3$. Here, $\sum_{m=-\infty}^{\infty}{}' \equiv \sum_{\substack{m=-\infty \\ (m\neq 0)}}^{\infty}$. We discuss the case $\alpha = 3$ later.

We consider a sinusoidal perturbation with wavenumber k in the x-direction of the form

$$(\delta x_m,\, \delta y_m) = (\xi,\, \eta)\mathrm{e}^{\mathrm{i}kma}. \tag{25}$$

Inserting (25) into (23) and (24), one obtains

$$\frac{\mathrm{d}}{\mathrm{d}t}\xi = -\frac{2\sigma}{a^{4-\alpha}}(\alpha-2)\Psi(\alpha)S(\alpha;ka)\eta, \tag{26}$$

$$\frac{\mathrm{d}}{\mathrm{d}t}\eta = -\frac{2\sigma}{a^{4-\alpha}}(3-\alpha)(\alpha-2)\Psi(\alpha)S(\alpha;ka)\xi, \tag{27}$$

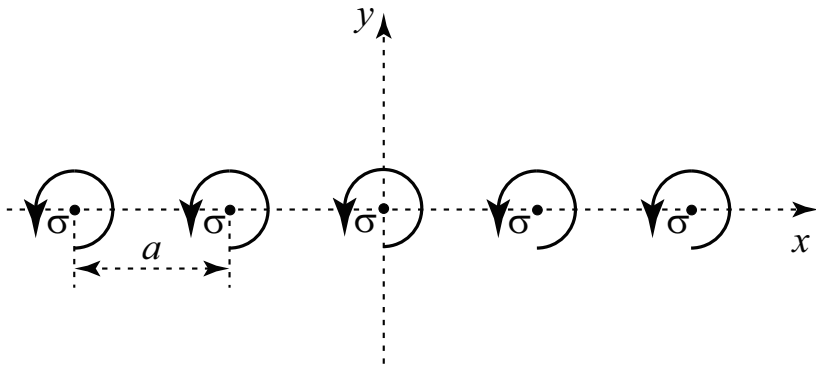

Figure 2. Infinite row of equidistant point vortices of equal strength σ.

where

$$S(\alpha; ka) \equiv \sum_{m=1}^{\infty} \frac{1-\cos kma}{m^{4-\alpha}}. \tag{28}$$

Equations (26) and (27) indicate that the perturbation exponentially grows as $(\xi,\, \eta) = (\xi_0,\, \eta_0)\mathrm{e}^{\Lambda t}$ with rate

$$\Lambda(\alpha; ka) = \sqrt{(3-\alpha)}\, \frac{2|\sigma|}{a^{4-\alpha}} (\alpha-2)\Psi(\alpha) S(\alpha; ka), \tag{29}$$

Here, $(\xi_0,\, \eta_0)$ is the amplitude of the initial perturbation.

First, we investigate the wavenumber dependence of the growth rate $\Lambda(\alpha; ka)$ under fixed values of α. To do this, we examine the ka-dependence of the infinite series $S(\alpha; ka)$ that appeared in (29). Although the case $\alpha = 0$ is meaningless for the generalized 2D fluid system‡, we discuss it to determine the asymptotic form of S for smaller values of α. The infinite series S can be expressed analytically for particular values of α as

$$S(0; ka) = \frac{\pi^4}{48} - \frac{1}{48}\left[2\pi^2 (ka-\pi)^2 - (ka-\pi)^4\right], \tag{30}$$

$$S(1; ka) = -\frac{(ka)^2}{2}\ln 2 - \int_0^{ka} (ka-t) \ln\left(\sin\frac{t}{2}\right) \mathrm{d}t, \tag{31}$$

$$S(2; ka) = \frac{1}{4} ka\,(2\pi - ka)\,. \tag{32}$$

Both $S(0; ka)$ and $S(1; ka)$ have zero slope at $ka = 0,\, \pi,\, 2\pi$ and maxima at $ka = \pi$. Moreover, $S(2; ka)$ is also maximum at $ka = \pi$. These are concave functions.

To investigate the dependence of S on ka generally, we need numerical calculations, because the infinite series S cannot be expressed analytically except for $\alpha = 0,\, 1,\, 2$ in the interval $0 \le \alpha \le 3$. In the numerical calculations, we approximate S as a Nth partial sum with sufficiently large N,

$$S_N(\alpha; ka) \equiv \sum_{m=1}^{N} \frac{1-\cos kma}{m^{4-\alpha}}. \tag{33}$$

‡ For $\alpha = 0$, the advection term in the governing equation $(1a)$ vanishes.

Figure 3 shows the dependence of S_N on ka for some values of α. Here, we set the upper bound for the summation (33) as $N = 10^6$. We have checked that the partial sums S_N shown in figure 3 converge within numerical errors, even for $N = 10^5$.

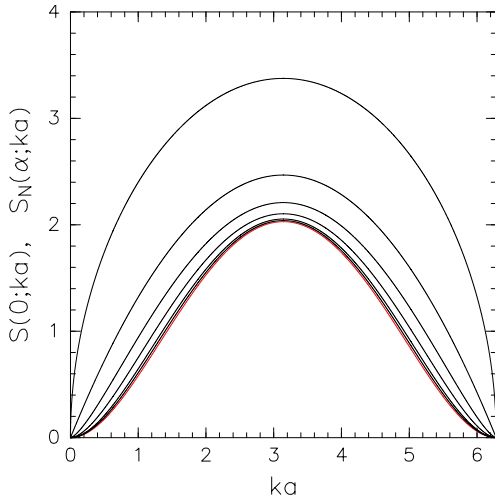

Figure 3. Partial sums $S_N(\alpha;\, ka)$ as a function of ka for some values of α, and the infinite sum $S(0; ka)$ as a function of ka. The black lines indicate S_N. From top to bottom, the black lines indicate the cases for $\alpha = 2.5$, 2, 1.5, 1, 0.5, 0.25. The red line indicates $S(0; ka)$. $S_N(0.25; ka)$ and $S_N(0.5; ka)$ almost collapse onto $S(0; ka)$ so that it is hard to distinguish them.

As indicated in figure 3, S_N (or equivalently S) are zero at $ka = 0$, 2π and maximum at $ka = \pi$. Therefore, when the values of α are fixed, the staggered perturbation ($ka = \pi$) is the fastest growing. This property is independent of the values of α. As α approaches zero, S converges to the functional form (30).

Next, we investigate the dependence of the growth rate (29) on α for the fastest growing mode ($ka = \pi$). In this case, the infinite series S reduces to

$$\begin{aligned} S(\alpha;\pi) &= \sum_{n=1}^{\infty} \frac{2}{(2n-1)^{4-\alpha}} \\ &= 2\left(1 - \frac{1}{2^{4-\alpha}}\right)\zeta(4-\alpha), \end{aligned} \tag{34}$$

where ζ is Riemann's ζ function, defined as [25],

$$\zeta(x) \equiv \sum_{n=1}^{\infty} \frac{1}{n^x}. \tag{35}$$

Therefore, we obtain

$$\Lambda(\alpha;\pi) = \sqrt{(3-\alpha)}\, \frac{4(2^{4-\alpha}-1)|\sigma|}{(2a)^{4-\alpha}} (\alpha - 2)\Psi(\alpha)\zeta(4-\alpha). \tag{36}$$

Figure 4 shows the dependence of the growth rate on α for the fastest growing mode. For numerical calculations of the growth rate, we replace the zeta function (35) by the

partial sum

$$\zeta_N(x) \equiv \sum_{n=1}^{N} \frac{1}{n^x}. \tag{37}$$

We set the upper bounds for the partial sum (37) as 10^5, 10^6, 10^7, 10^8, and 10^9. As shown in figure 4, the numerical values of the growth rate converge for $\alpha \lesssim 2.5$. However, for $\alpha \gtrsim 2.7$, the convergence of the numerical calculations worsens. We therefore estimate the growth rate in the vicinity of $\alpha = 3$ as follows. It is known that Riemann's zeta function has the asymptotic form

$$\lim_{x \to 1} \left(\zeta(x) - \frac{1}{x-1} \right) = \gamma, \tag{38}$$

where γ is Euler's constant [25],

$$\begin{aligned} \gamma &\equiv \lim_{n \to \infty} \left(1 + \frac{1}{2} + \frac{1}{3} + \cdots + \frac{1}{n} - \ln n \right) \\ &= 0.577\,215\,664\,901\,532\ldots \end{aligned} \tag{39}$$

Therefore, we estimate Riemann's zeta function as

$$\zeta(4-\alpha) \approx \frac{1}{3-\alpha} + \gamma \tag{40}$$

for $\alpha \geq 2.6$. Then, the growth rate (36) with (40) is shown in figure 4 by the red line. As indicated by the figure, the growth rates with the partial sum tend to approach the theoretical estimate as N increases. Therefore, the growth rate is well estimated by (36) with (40) in the vicinity of $\alpha = 3$.

We summarize the linear stability of the infinite row of equidistant point vortices of equal strength for $0 < \alpha < 3$. The row of vortices is unstable in the sense that sinusoidal perturbations to the vortex positions grow exponentially with time. The growth rate is a function of α and the wavenumber of the perturbation. The staggered perturbation is the fastest growing perturbation irrespective of the values of α. As $\alpha \to 0$, the growth rate vanishes. In contrast, the growth rate for the fastest growing perturbation increases as $\Lambda(\alpha;\pi) \sim (3-\alpha)^{-1/2}$ as $\alpha \to 3$. However, the dependence of the growth rate of the fastest growing perturbation on α is not a monotonic increasing function of α, as shown in figure 4. Except for the vicinity of $\alpha = 3$, the dependence of $\Lambda(\alpha;\pi)$ on α is mainly responsible for the functional form of the coefficient $(2-\alpha)\Psi(\alpha)$ (see figure 1).

In the case $\alpha = 3$, we must go back to (23) and (24). Although (23) does not change, (24) is replaced by

$$\frac{\mathrm{d}}{\mathrm{d}t}\delta y_0 = 0. \tag{41}$$

Moreover, (26) and (27) reduce to

$$\frac{\mathrm{d}}{\mathrm{d}t}\xi = -\frac{\sigma}{\pi a} S(3;ka)\eta, \tag{42}$$

$$\frac{\mathrm{d}}{\mathrm{d}t}\eta = 0. \tag{43}$$

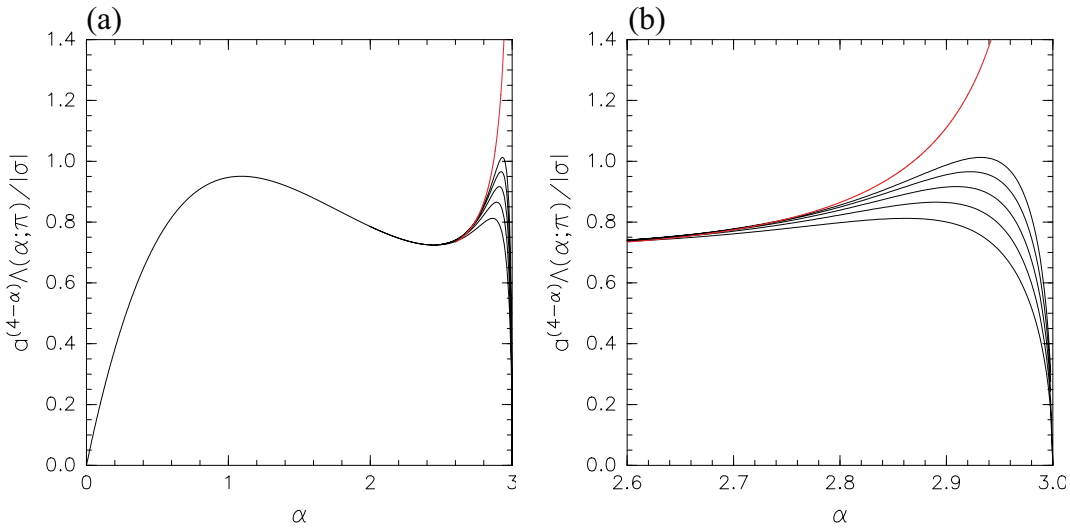

Figure 4. The left panel (a) indicates dependence of the growth rate $\Lambda(\alpha;\pi)$ on α for the fastest growing mode. The black lines indicate Λ, (36), where the zeta functions are replaced by the partial sum (37). The upper bounds for the partial sum (37) are set $N = 10^9$, 10^8, 10^7, 10^6, 10^5, shown from top to bottom. The red line indicates the growth rate in the case where the zeta function is estimated by (40). The right panel (b) is the same as the left panel but the region $\alpha \geq 2.6$ is enlarged.

Thus, the perturbation remains unchanged in the y-direction but grows algebraically with time in the x-direction as $\xi = -\lambda t + \xi_0$, where $\lambda = \sigma S(3; ka)\eta_0/(\pi a)$ and (ξ_0, η_0) is the initial perturbation. For $ka = 0$ and 2π, $S(3; ka) = 0$. However, except for those values, $S(3; ka)$ is a divergent series. Thus, the growth rate λ is infinite.

4. Linear stability of a sheet vortex

Taking the limit of the distance between the vortices $a \to 0$ in the results of the previous section, we discuss the stability of a sheet vortex for the generalized 2D fluid system. First, we calculate the flows induced by an unperturbed sheet vortex (the basic state velocities for a sheet vortex instability problem), because they have not been studied yet.

4.1. Flow induced by an unperturbed sheet vortex

The azimuthal velocity induced by a point vortex with unit strength located at (x_0, y_0) is given by [20]

$$v_\phi(x, y; x_0, y_0) = \frac{(\alpha - 2)\Psi(\alpha)}{\left(\sqrt{(x - x_0)^2 + (y - y_0)^2}\right)^{3-\alpha}}. \tag{44}$$

Suppose that a sheet vortex with a strength of the line density ρ is placed on the x-axis. We estimate the x-component of the velocity induced by the sheet vortex as a function of y (see figure 5). From the symmetry of the system, we may calculate the x-component

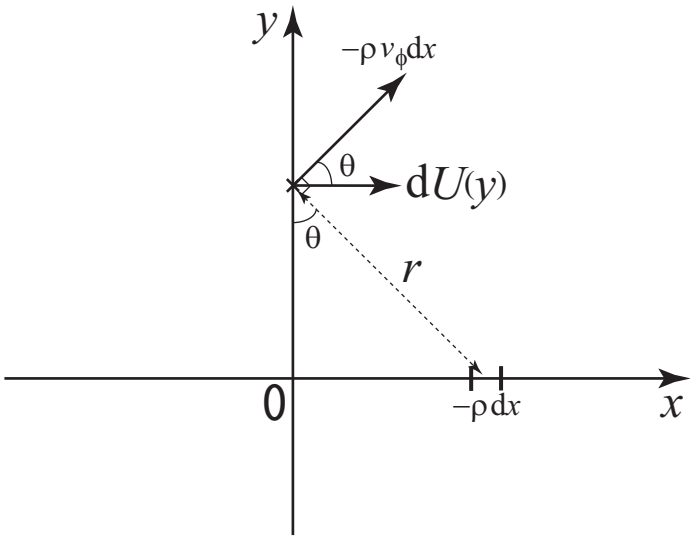

Figure 5. x-component of the velocity, apart from the x-axis, induced by a sheet vortex with a strength of the line density $-\rho$ placed on the x-axis.

of the velocity at $(0,\, y)$ without loss of generality. Then, we have

$$U(y) = -\rho\ \mathrm{sgn}(y) \int_{-\infty}^{\infty} v_\phi(0, y; x, 0) \cos\theta\, \mathrm{d}x, \tag{45}$$

where $\mathrm{sgn}(y)$ is the signum function, defined by

$$\mathrm{sgn}(y) = \begin{cases} 1, & (y > 0) \\ 0, & (y = 0) \\ -1, & (y < 0) \end{cases} \tag{46}$$

and $\tan\theta \equiv x/y$. Inserting (44) into (45), and transforming the variable from x to θ, we obtain

$$\begin{aligned} U(y) &= -\rho\ \mathrm{sgn}(y)(\alpha-2)\Psi(\alpha)|y|^{\alpha-2} \int_{-\pi/2}^{\pi/2} \cos^{2-\alpha}\theta\, \mathrm{d}\theta \\ &= -\rho\ \mathrm{sgn}(y)(\alpha-2)\Psi(\alpha) B\left(\frac{1}{2}, \frac{3-\alpha}{2}\right)|y|^{\alpha-2} \\ &= -\rho\ \mathrm{sgn}(y) V(\alpha)|y|^{\alpha-2}, \end{aligned} \tag{47}$$

$$V(\alpha) \equiv \frac{1}{2^{\alpha-1}\sqrt{\pi}} \frac{\Gamma\left(\frac{3-\alpha}{2}\right)}{\Gamma\left(\frac{\alpha}{2}\right)}, \tag{48}$$

where $B(m, n)$ is the beta function, defined by

$$B(m,\, n) \equiv 2\int_0^{\pi/2} \sin^{2m-1}\theta \cos^{2n-1}\theta\, \mathrm{d}\theta. \tag{49}$$

The last expression of (47) is derived with the aid of the relation between the beta and gamma functions,

$$B(m, n) = \frac{\Gamma(m)\Gamma(n)}{\Gamma(m+n)}, \tag{50}$$

and (17). Figure 6 shows the dependence of V on α. The coefficient V is a monotonic increasing function of α, and diverges as α approaches 3.

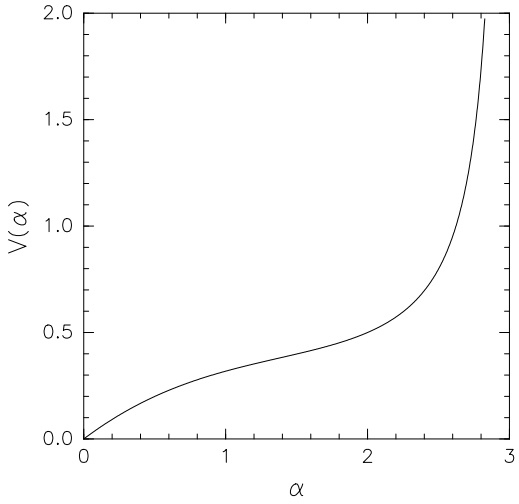

Figure 6. $V(\alpha)$ as a function of α.

The velocity U induced by the sheet vortex depends algebraically on $|y|$. It diverges as the sheet vortex is approached for $\alpha < 2$. In contrast, for $\alpha > 2$, it converges to zero as the sheet vortex is approached, and increases away from the sheet vortex (see figure 7). In other words, the sheet vortex ($y = 0$) is a singular point for the velocity U for $\alpha \leq 2$, but not for $\alpha > 2$. For $\alpha = 3$, the velocity U is a linear function of y. However, the proportional constant is infinite. Because the magnitude of the velocity induced by the point vortex for $\alpha = 3$ is independent of the distance from the vortex (cf. (44) with $\alpha = 3$), an infinite length of sheet vortex on the x-axis produces an infinite speed. The basic state velocity for $\alpha = 3$ is infinite everywhere in the flow domain except for $y = 0$. It would be inappropriate to examine the stability of such basic state. Thus, we exclude the case $\alpha = 3$ in the following discussion.

For $\alpha = 1$, 2, the velocity U can be expressed analytically as

$$U(y) = -\mathrm{sgn}(y)\,\frac{\rho}{\pi|y|}, \quad (\alpha = 1), \tag{51}$$

$$U(y) = -\mathrm{sgn}(y)\,\frac{\rho}{2}, \qquad (\alpha = 2). \tag{52}$$

Equation (52) is the well-known velocity profile for a KH instability problem for the 2D Euler system.

4.2. Growth rate of a perturbation applied to the sheet vortex

The stability analysis of the row of point vortices in section 3.2 implies that the sheet vortex is unstable. We derive the exponential growth rate of a sinusoidal perturbation applied to the sheet vortex by taking the limit $a \to 0$ in the exponential growth rate of a sinusoidal perturbation applied to the row of vortices obtained in section 3.2. From (28)

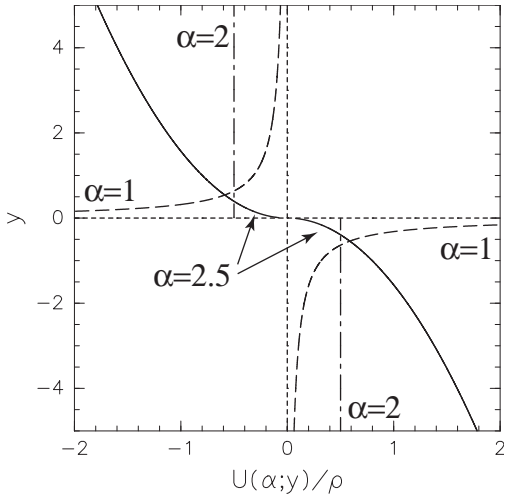

Figure 7. Velocity induced by a sheet vortex placed on the x-axis. The cases $\alpha = 1$, 2, 2.5 are shown.

and (29), the exponential growth rate of a perturbation applied to the row of vortices Λ can be rewritten as

$$\Lambda(\alpha; ka) = \frac{|\sigma|}{a}\sqrt{3-\alpha}\,(\alpha-2)\Psi(\alpha)\sum_{m=-\infty}^{\infty}{}' a\frac{1-\cos kma}{(|m|a)^{4-\alpha}}, \tag{53}$$

for $0 < \alpha < 3$. When taking the limit $a \to 0$, the strength of the sheet vortex of unit length $|\sigma|/a$ remains a finite $|\rho|$ ($|\rho| \equiv |\sigma|/a$). Moreover, in this limit, we can replace ma with x and $\sum'_{m=-\infty}^{\infty} a \to \mathcal{P}\int_{-\infty}^{\infty} \mathrm{d}x$. Then, we have an exponential growth rate for a sinusoidal perturbation applied to the sheet vortex

$$\begin{aligned}\Lambda(\alpha; k) &= |\rho|\sqrt{(3-\alpha)}\,(\alpha-2)\Psi(\alpha)\,\mathcal{P}\int_{-\infty}^{\infty}\frac{1-\cos kx}{|x|^{4-\alpha}}\,\mathrm{d}x \\ &= 2|\rho|\sqrt{(3-\alpha)}\,(\alpha-2)\Psi(\alpha)I(\alpha)k^{3-\alpha}, \qquad (54)\\ I(\alpha) &= \mathcal{P}\int_0^{\infty}\frac{1-\cos x}{x^{4-\alpha}}\,\mathrm{d}x, \qquad (55)\end{aligned}$$

for $0 < \alpha < 3$, where $\mathcal{P}$ indicates the Cauchy principle value.

The growth rate converges or diverges depending on the value of α. The integral (55) reduces to a different kind of improper integral depending on the value of α. The integrand of (55) behaves as $x^{\alpha-2}$ as x approaches zero. Thus, the integrand has no singular points for $2 \le \alpha < 3$, and the integral (55) for $2 \le \alpha < 3$ is an improper integral of the first kind. In contrast, for $0 < \alpha < 2$, the integrand of (55) is singular at $x = 0$ and the integral (55) is an improper integral of the third kind. From theorems on the convergence of improper integrals [26], the integral (55) converges for $1 < \alpha < 3$ and diverges for $0 < \alpha \le 1$. In other words, a transition of the growth rate of the perturbation occurs at $\alpha = 1$. Divergence of the growth rate for $\alpha \le 1$ does not arise in the case of instability of the row of vortices, as discussed in the previous section. Hence, the transition of the growth rate at $\alpha = 1$ is a peculiar property of continuous distributions of the generalized vorticity.

Alternatively, we can derive the transition of the growth rate at $\alpha = 1$ from the asymptotic behavior of $S(\alpha; ka)$ for smaller ka. The factor $|\sigma|/a^{4-\alpha}$ in the growth rate (29) can be divided into $|\sigma|/a \times a^{\alpha-3}$. We take the limit $a \to 0$ while keeping the first part of the factor constant $|\rho| = |\sigma|/a$, as in the previous discussion. Then, for the growth rate to be finite, the infinite sum $S(\alpha; ka)$ must behave as $S(\alpha; ka) \sim (ka)^{3-\alpha}$ for smaller ka. Otherwise, the growth rate diverges or converges to zero as $a \to 0$. We therefore examine the asymptotic behavior of $S(\alpha; ka)$ (equivalently, $S_N(\alpha; ka)$) for smaller ka for several values of α in figure 8. Here, we set $N = 10^6$ as the upper bound for S_N, as before. For comparison, the reference lines $(ka)^{3-\alpha}$ for $\alpha = 2.5$, 2, 1.5, 1 are also shown in figure 8. Figure 8 shows that $S_N(\alpha; ka)$ for $\alpha = 2.5$, 2, 1.5 behaves as $S_N \sim (ka)^{3-\alpha}$. However, for $\alpha = 1$, 0.5, 0.25, S_N deviates from the form $S_N \sim (ka)^{3-\alpha}$. In the case of $\alpha = 0.5$, 0.25, it seems that the values of S_N are saturated by $S_N \sim (ka)^2$. In the case of $\alpha = 1$, we can calculate

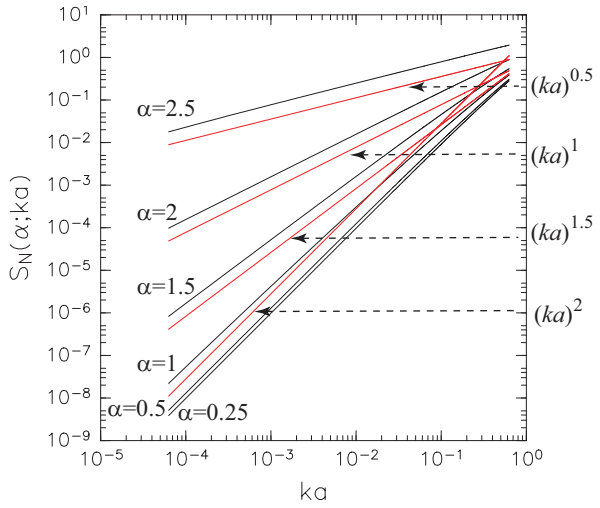

Figure 8. $S_N(\alpha; ka)$ (black lines) for $\alpha = 2.5$, 2, 1.5, 1, 0.5, 0.25 from top to bottom. The red lines indicate the reference lines $(ka)^{0.5}$, $(ka)^1$, $(ka)^{1.5}$, $(ka)^2$.

$$S(1; ka) = -\frac{(ka)^2}{2} \ln ka + \frac{3}{4}(ka)^2 + \mathrm{O}\left((ka)^4\right) \tag{56}$$

from (31) for $ka \ll 1$. Therefore, the term proportional to $(ka)^{3-\alpha} (= (ka)^2)$ in $S_N(1; ka)$ is $S_N(1; ka) \sim (\frac{3}{4} - \ln ka)(ka)^2$. Figure 9 shows the dependence of $S_N(1; ka)$ on ka and the reference line $-(\ln ka)(ka)^2$. It indicates that the above estimate is valid. As α becomes smaller, $S(\alpha; ka)$ approaches $S(0; ka)$. Equation (30) indicates that the leading order of $S(0; ka)$ is $S(0; ka) \sim (ka)^2$. Thus, figure 8 is consistent with this fact. The asymptotic behavior of S_N (equivalently, S) at small ka leads to divergence of the growth rate of the sheet vortex perturbation for $\alpha \leq 1$. In particular, it shows a logarithmic divergence of the growth rate at $\alpha = 1$.

The instability of the sheet vortex for $\alpha = 2$ considered here is just a KH instability for the 2D Euler system. The growth rate (54) for $\alpha = 2$ is consistent with that of a

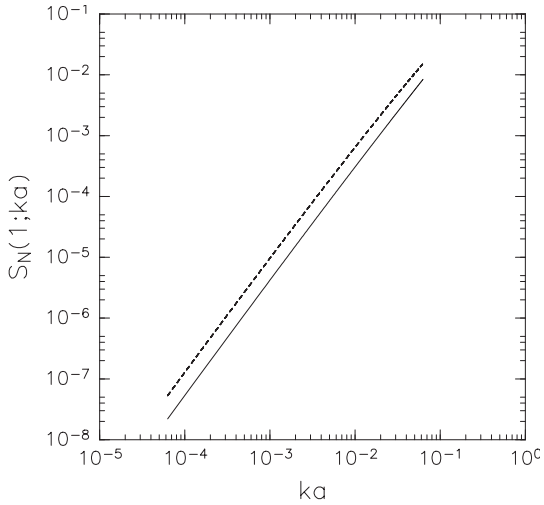

Figure 9. $S_N(1;ka)$ (solid line) and the reference $\{-\ln(ka)\}\,(ka)^2$ (dashed line).

KH instability for the 2D Euler system. The integral that appeared in (54) for $\alpha = 2$ reduces to

$$I(2) = \int_0^\infty \frac{1-\cos x}{x^2}\,\mathrm{d}x = \frac{\pi}{2}. \tag{57}$$

Thus, we have the growth rate

$$\Lambda(2;k) = \frac{|\rho|}{2}k. \tag{58}$$

Furthermore, using (52), (58) can be written in terms of the basic state velocity U as

$$\Lambda(2;k) = |U|k. \tag{59}$$

This is just the growth rate of the perturbation for a KH instability problem for the 2D Euler system [23].

5. Discussion

Equation (54) indicates that the growth rate of the perturbation depends on the wavenumber as $\Lambda \sim k^{3-\alpha}$. This result can be derived by the following dimensional analysis. Suppose that the growth rate depends on the strength of the line density of the sheet vortex $|\rho|$ and the wavenumber k. Then, the dimensions of σ and ρ are

$$[\sigma] = [q] \times L^2 = L^{4-\alpha}T^{-1},$$
$$[\rho] = \frac{[\sigma]}{L} = L^{3-\alpha}T^{-1},$$

respectively. Therefore, dimensional analysis leads to $\Lambda \sim |\rho|k^{3-\alpha}$. In the case $\alpha = 2$, a dimensional analysis based on the basic state velocity U and the wavenumber k, and that based on the strength of the line density of the sheet vortex (ρ) and k lead to the same result for the dependence of the growth rate on k. However, the above analysis

implies that the strength of the line density of the sheet vortex is a more fundamental quantity than the basic state velocity U.

As stated in section 4.1, $\alpha = 2$ is a transition point of the basic state velocity U, in the sense that the velocity U diverges as $y \to 0$ for $\alpha < 2$. If the velocity U were a fundamental quantity for the instability of the sheet vortex, $\alpha = 2$ would be a transition point for the growth rate Λ. However, we can prove that the growth rate Λ is continuous at $\alpha = 2$. The factor $(\alpha - 2)\Psi(\alpha)$ that appears in (54) is a continuous function of α in the interval $0 < \alpha < 3$ (see figure 1). Moreover, the integral $I(\alpha)$, (55), is continuous at $\alpha = 2$ because

$$\left[\frac{\mathrm{d}}{\mathrm{d}\alpha}\int_0^\infty \frac{1-\cos x}{x^{4-\alpha}}\,\mathrm{d}x\right]_{\alpha=2} = \int_0^\infty \frac{1-\cos x}{x^2}\ln x\,\mathrm{d}x = -\frac{1}{2}(\gamma-1)\pi, \tag{60}$$

where γ is Euler's constant (given by (39)). Therefore, the growth rate Λ is continuous at $\alpha = 2$, and thus the transition of the growth rate does not occur at $\alpha = 2$. This implies that the basic state velocity is a less fundamental quantity for the instability than the strength of the line density of the sheet vortex.

The mechanism of the instability of a sheet vortex for the 2D Euler system can be understood in terms of the changes in the vorticity distribution and the consequent effect on the velocity distribution [27]. This mechanism could be applied to the generalized 2D fluid system. A schematic diagram of the instability mechanism of the sheet vortex is shown in figure 10. Suppose that the sheet vortex is perturbed sinusoidally as $\eta = \eta_0 \mathrm{e}^{\mathrm{i}kx}$, as shown in figure 10. The generalized vorticity is advected by the basic flow U towards point A where $\eta = 0$ and $\partial_x \eta > 0$, and away from point B where $\eta = 0$ and $\partial_x \eta < 0$. As a result, the generalized vorticity densities at A and B are thicker and thinner, respectively. This leads to a perturbation generalized vorticity distribution of the form $\delta(y)\mathrm{e}^{\mathrm{i}kx}$ along the x-axis. The resulting generalized vorticity distribution induces anticlockwise and clockwise velocities around A and B, respectively. The induced velocities amplify the perturbation of the sheet vortex further, leading to instability.

We confirm our model of sheet vortex instability. First, according to the model, we calculate the perturbation stream function for the sheet vortex instability problem to investigate the dependence of the spatial structure of the stream function on α. In particular, we are interested in the y-dependence of the perturbation stream function. It is obvious that the x-dependence of the perturbation stream function is sinusoidal $\mathrm{e}^{\mathrm{i}kx}$, because the perturbation applied to the sheet vortex is proportional to $\mathrm{e}^{\mathrm{i}kx}$. As explained in the previous paragraph, the perturbed generalized vorticity for the unstable perturbation is distributed along the x-axis in the form $\delta(y)\mathrm{e}^{\mathrm{i}kx}$. Therefore, we solve an equation of the form

$$-(-\Delta)^{\alpha/2}\psi' = \epsilon\delta(y)\mathrm{e}^{\mathrm{i}kx}, \tag{61}$$

where ϵ is a complex amplitude. Now, we suppose $k > 0$ without loss of generality. We solve (61) by expressing ψ' as a monochromatic wave of wavenumber k with respect to x

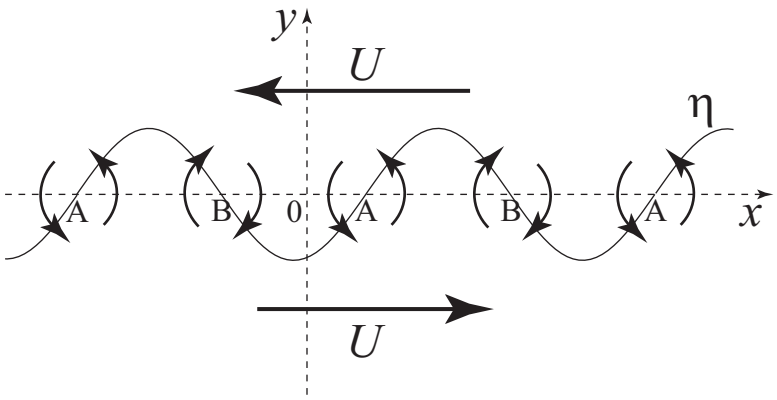

Figure 10. Schematic diagram of a mechanism for sheet vortex instability. The thin solid line indicates the perturbed sheet vortex. The basic flow U advects the generalized vorticity. The anticlockwise and clockwise circular arrows indicate the velocities induced by the perturbed generalized vorticity centered at A and B, respectively.

and as a Fourier transformation with respect to y. We express the perturbation stream function ψ' by

$$\psi'(x,y) = \frac{1}{\sqrt{2\pi}} \int_{-\infty}^{\infty} \hat{\psi}'(k,l) \mathrm{e}^{\mathrm{i}(kx+ly)} \, \mathrm{d}l. \tag{62}$$

Then, (61) reduces to

$$\hat{\psi}'(k,l) = -\frac{\epsilon}{\sqrt{2\pi}} \frac{1}{(k^2+l^2)^{\alpha/2}}. \tag{63}$$

With the aid of a formula for the Fourier transform (B.7), we find

$$\psi' = -\frac{\epsilon}{\sqrt{\pi}\Gamma(\alpha/2)} \left(\frac{|y|}{2k}\right)^{(\alpha-1)/2} K_{\frac{\alpha-1}{2}}(k|y|) \, \mathrm{e}^{\mathrm{i}kx}, \tag{64}$$

where $K_\nu(y)$ is a modified Bessel function of the second kind of order ν. (Note that the Bessel function formulae necessary for the present study are listed in Appendix B.) Therefore, the y-dependence of the perturbation stream function for sheet vortex instability in the generalized 2D fluid system is given by a multiple of a power function and a modified Bessel function of the second kind.

Next, we show that (64) reduces to the perturbation stream function for a KH instability for the 2D Euler system of the form $\mathrm{e}^{\mathrm{i}kx-k|y|}$ [23]. From the definition of Bessel functions, the Bessel function of the second kind of order $\frac{1}{2}$ is given by (B.4). Thus, with the aid of (B.4), (64) with $\alpha = 2$ leads to

$$\begin{aligned} \psi' &= -\frac{\epsilon}{\sqrt{\pi}\Gamma(1)} \left(\frac{|y|}{2k}\right)^{1/2} K_{\frac{1}{2}}(k|y|) \, \mathrm{e}^{\mathrm{i}kx} \\ &= -\frac{\epsilon \mathrm{e}^{\mathrm{i}kx-k|y|}}{2k}. \end{aligned} \tag{65}$$

Therefore, (65) is consistent with the perturbation stream function for a KH instability for the 2D Euler system, except for a proportionality constant.

Once the perturbation stream function is obtained, we can determine the induced velocity due to the perturbed sheet vortex. In particular, we concentrate our attention on the y-component of the velocity v', which is calculated by $v' = \partial_x \psi'$. Because the perturbation stream function behaves as $\mathrm{e}^{\mathrm{i}kx}$ in the x-direction, the y-component of the perturbation velocity is $\mathrm{i}k\psi'$ and the y-dependence of the velocity v' is equivalent to that of the perturbation stream function. We examine the behavior of v' at $y = 0$, which indicates the y-component of an induced velocity on the perturbed sheet vortex within a linear approximation. With the aid of the formula for Bessel functions of the second kind given a small argument, (B.5), and (64), the perturbation velocity v' for $\alpha \neq 1$ is given by

$$\begin{aligned} v' &\sim \frac{\mathrm{i}k\pi}{2\sin\left(\frac{|\alpha-1|}{2}\pi\right)\Gamma\left(1-\frac{|\alpha-1|}{2}\right)}(k|y|)^{(\alpha-1)/2}\left(\frac{2}{k|y|}\right)^{|\alpha-1|/2}\mathrm{e}^{\mathrm{i}kx} \\ &\sim \frac{\mathrm{i}2^{|\alpha-1|/2-1}k\pi}{\sin\left(\frac{|\alpha-1|}{2}\pi\right)\Gamma\left(1-\frac{|\alpha-1|}{2}\right)}(k|y|)^{\{(\alpha-1)-|\alpha-1|\}/2}\mathrm{e}^{\mathrm{i}kx}. \end{aligned} \tag{66}$$

This shows that the asymptotic form of the perturbation velocity v' is independent of y for $\alpha > 1$, but proportional to the negative power of $|y|$ for $\alpha < 1$. This indicates that the perturbation velocity v' remains finite for $\alpha > 1$, but diverges for $\alpha < 1$ at $y = 0$. For $\alpha = 1$, (64) leads to

$$v' \sim \mathrm{i}kK_0(k|y|)\mathrm{e}^{\mathrm{i}kx} \sim \mathrm{i}k\left(\ln\frac{2}{k|y|} - \gamma\right)\mathrm{e}^{\mathrm{i}kx} \tag{67}$$

with the aid of (B.6). Therefore, v' for $\alpha = 1$ diverges logarithmically as $y \to 0$. An infinite velocity v' could amplify the perturbed sheet vortex at infinite speed. The finiteness of the perturbation velocity v' on the sheet vortex as a function of α is consistent with that of the growth rate Λ of the perturbation to the sheet vortex discussed in the previous section. This indicates the validity of our mechanism for sheet vortex instability.

We have not discussed the instability of the sheet vortex for $\alpha = 3$. However, it is easily inferred from that of the point vortex street. For $\alpha = 3$, the perturbation applied to the point vortex street algebraically grows and its growth rate λ is infinite. Thus, the growth of the perturbation to the sheet vortex for $\alpha = 3$ is algebraic and their rate is infinite. This singular behavior of the growth rate at $\alpha = 3$ originates from the infinite length of the sheet vortex along the x-axis. In contrast, the singularity of the exponential growth rate Λ for $\alpha \leq 1$ is caused by the infinitesimal thickness of the sheet vortex, because the above analysis indicates that the singularity of Λ for $\alpha \leq 1$ arises from the divergence of v' on the sheet vortex, namely $\lim_{y\to 0} v' \to \infty$. Thus, this raises the question of whether the growth rate of perturbations applied to a vortex layer with finite thickness, *e.g.* (12) or (13), diverges for $\alpha \leq 1$. To respond to this question, we need further analysis of such basic states. The analysis would require numerical calculations. The numerical analysis of the instability of such vorticity profile will be investigated in a forthcoming paper.

6. Summary

We discussed the linear stability of parallel shear flows for the inviscid generalized 2D fluid system. First, we derived a sufficient condition for the stability of parallel shear flows through a wave activity conservation law. The derived sufficient condition for stability is a generalization of Rayleigh's criterion for the 2D Euler system to the generalized 2D fluid system. The generalization is naive in the sense that the vorticity gradient in the criterion for the 2D Euler system generalizes to the generalized vorticity gradient. Next, we discussed the linear stability of a sheet vortex. A sheet vortex is a simple but fundamental flow that violates the stability criterion. The generalized vorticity profile whose stability was investigated was the same as the vorticity profile of a KH instability problem for the 2D Euler system. In this sense, we investigated a KH instability for the generalized 2D fluid system in this paper. We examined the stability of an infinite row of equidistant point vortices of equal strength first, and then took the limit of the distance between the vortices to zero in order to consider the stability of a sheet vortex. The row of point vortices was unstable in the sense that a sinusoidal perturbation applied to the row of vortices grew exponentially with time, except when $\alpha \neq 3$. For $\alpha = 3$, the row of vortices was also unstable, but the applied perturbation grew algebraically with time. However, due to the intrinsic nature of the point vortices for $\alpha = 3$, the growth rate of the perturbation was infinite. The basic state velocity induced by the sheet vortex for $\alpha = 3$ was infinite almost everywhere in the flow domain. Therefore, we excluded the case $\alpha = 3$ in the examination of sheet vortex stability. The sheet vortex was also unstable in the sense that the sinusoidal perturbation applied to the sheet vortex grew exponentially with time. The growth rate Λ was finite and depended on the wavenumber as $\Lambda \sim k^{3-\alpha}$ for $1 < \alpha < 3$. However, for $\alpha \leq 1$, the growth rate was infinite. In other words, there was a transition in the growth rate at $\alpha = 1$. We have shown that the physical model of sheet vortex instability for the 2D Euler system also worked well for the generalized 2D fluid system. We proposed a physical model for KH instability in the generalized 2D fluid system and explained the transition of the growth rate of the perturbation at $\alpha = 1$ using it.

It is well known that the Rayleigh stability condition for the 2D Euler system is valid not only for a linear perturbation of the basic state, but also for a finite-amplitude perturbation [28]. In this sense, we can anticipate that the basic state satisfying the generalized Rayleigh stability condition which was just derived in this study is nonlinearly stable. The proof of nonlinear stability for the 2D Euler system relies on the existence of the Hamiltonian, Casimir, and Impulse, i.e., a Hamilton structure for the 2D Euler system. Thus, derivations of the Hamilton structure for the generalized 2D fluid system and nonlinear stability criteria for parallel shear flows should be subjects for future study. Here, we derived Rayleigh's stability condition for the generalized 2D fluid system. It is well-known for the 2D Euler system that another stability condition exists (Fjørtoft's criterion). The generalization of Fjørtoft's criterion to the generalized 2D fluid system is also a subject for future study.

Acknowledgments

This work was supported by a Grant-in-Aid for Scientific Research (C) No. 24540472 from the Japanese Society for the Promotion of Science. This study was also partly supported by the Center for Planetary Science (CPS) running under the auspices of the MEXT GCOE Program "Foundation of the International Center for Planetary Science". T. I. thanks Prof. Y.-Y. Hayashi, Drs. K. Yamazaki and T. Yajima of Kobe University, and all members of the Atmospheric Science group of Kobe University for helpful conversations on this topic. The GFD-DENNOU Library was used for drawing figures.

Appendix A. Derivation of (7)

Here, we present a derivation of (7) in the case of a periodic domain with dimensions $[-L, L]\times[-D, D]$. The kinematic relation between the stream function and the vorticity $(1b)$ reduces to

$$\hat{q}(\boldsymbol{k}) = -|\boldsymbol{k}|^{\alpha}\hat{\psi}(\boldsymbol{k}), \tag{A.1}$$

where $\hat{q}(\boldsymbol{k})$ and $\hat{\psi}(\boldsymbol{k})$ are the Fourier components of q' and ψ', respectively. The Fourier components of $f(\boldsymbol{r})$ (which is an arbitrary function of $\boldsymbol{r} = (x, y)$) are given by

$$\hat{f}(\boldsymbol{k}) = \frac{1}{4LD}\int_{\Omega} f(\boldsymbol{r})\mathrm{e}^{-i\boldsymbol{k}\cdot\boldsymbol{r}}\mathrm{d}\boldsymbol{r}, \quad f(\boldsymbol{r}) = \sum_{\boldsymbol{k}} \hat{f}(\boldsymbol{k})\mathrm{e}^{\mathrm{i}\boldsymbol{k}\cdot\boldsymbol{r}}. \tag{A.2}$$

Here, we use the notation

$$\int_{\Omega} f\,\mathrm{d}\boldsymbol{r} \equiv \int_{-L}^{L}\int_{-D}^{D} f\,\mathrm{d}x\mathrm{d}y, \quad \sum_{\boldsymbol{k}} \equiv \sum_{m=-\infty}^{\infty}\sum_{n=-\infty}^{\infty}, \tag{A.3}$$

where $\boldsymbol{k} = (k, l) = (\pi m/L, \pi n/D)$. We have

$$\begin{aligned}
\int_{\Omega} \frac{\partial\psi'}{\partial x} q'\,\mathrm{d}\boldsymbol{r} &= \int_{\Omega} q'\frac{\partial}{\partial x}\left(\sum_{\boldsymbol{k}} \hat{\psi}(\boldsymbol{k})\mathrm{e}^{\mathrm{i}\boldsymbol{k}\cdot\boldsymbol{r}}\right)\mathrm{d}\boldsymbol{r} \\
&= \sum_{\boldsymbol{k}} \mathrm{i}k\hat{\psi}(\boldsymbol{k})\int_{\Omega} q'\mathrm{e}^{\mathrm{i}\boldsymbol{k}\cdot\boldsymbol{r}}\,\mathrm{d}\boldsymbol{r} \\
&= 4LD\sum_{\boldsymbol{k}} \mathrm{i}k\hat{\psi}(\boldsymbol{k})\hat{q}(-\boldsymbol{k}) \\
&= 4LD\sum_{\boldsymbol{k}} \mathrm{i}k\hat{\psi}(\boldsymbol{k})(-|\boldsymbol{k}|^{\alpha})\hat{\psi}(-\boldsymbol{k}) \\
&= 4LD\sum_{\boldsymbol{k}} \mathrm{i}k\hat{q}(\boldsymbol{k})\hat{\psi}(-\boldsymbol{k}) \\
&= \sum_{\boldsymbol{k}} \mathrm{i}k\hat{q}(\boldsymbol{k})\int_{\Omega} \psi'\mathrm{e}^{\mathrm{i}\boldsymbol{k}\cdot\boldsymbol{r}}\mathrm{d}\boldsymbol{r} \\
&= \int_{\Omega} \psi'\frac{\partial q'}{\partial x}\,\mathrm{d}\boldsymbol{r}.
\end{aligned} \tag{A.4}$$

To derive the fourth and fifth equality, we use (A.1).

If the domain is a zonal channel with dimensions $[-L, L] \times [0, D]$, $\psi'(\boldsymbol{r})$ is expanded as

$$\psi' = \sum_{\substack{m=-\infty \\ (m\neq 0)}}^{\infty} \sum_{n=1}^{\infty} \hat{\psi}(m,n) \mathrm{e}^{\mathrm{i}kx} \sin(ly), \tag{A.5}$$

where $(k, l) = (\pi m/L, \pi n/D)$. From the kinematic relation $(1b)$ and (A.5), we have

$$q' = \sum_{\substack{m=-\infty \\ (m\neq 0)}}^{\infty} \sum_{n=1}^{\infty} -\left(k^2 + l^2\right)^{\alpha/2} \hat{\psi}(m,n) \mathrm{e}^{\mathrm{i}kx} \sin(ly). \tag{A.6}$$

On the other hand, if the domain is infinite, q and ψ are expressed in terms of a Fourier transformation. The derivations of (7) in these cases are similar to the derivation in the case of a doubly periodic domain.

Appendix B. Bessel function formulae

Formulae for Bessel functions necessary for the present paper are listed in the following. The definition of a modified Bessel function of the second kind depends on the literature [25, 29]. In this study, we follow the definition of Watson [29].

Appendix B.1. Definitions of Bessel functions

Bessel function of the first kind

$$J_\nu(x) \equiv \left(\frac{x}{2}\right)^\nu \sum_{m=0}^{\infty} \frac{(-1)^m}{m!\,\Gamma(m+1+\nu)} \left(\frac{x}{2}\right)^{2m}. \tag{B.1}$$

Modified Bessel function of the first kind

$$I_\nu(x) \equiv i^{-\nu} J_\nu(ix). \tag{B.2}$$

Modified Bessel function of the second kind

$$K_\nu(x) \equiv \frac{\pi}{2} \frac{I_{-\nu}(x) - I_\nu(x)}{\sin(\nu\pi)}. \tag{B.3}$$

It has a property of $K_\nu = K_{-\nu}$.

Appendix B.2. Modified Bessel function of the second kind of the order $\nu = \pm\frac{1}{2}$

$$K_{\frac{1}{2}}(x) = K_{-\frac{1}{2}}(x) = \sqrt{\frac{\pi}{2x}} \mathrm{e}^{-x}. \tag{B.4}$$

Appendix B.3. Asymptotic form of the modified Bessel function of the second kind for $x \to 0$

For the order $\nu \neq 0$,

$$K_\nu(x) \sim \frac{\pi}{2\sin(|\nu|\pi)\Gamma(1-|\nu|)} \left(\frac{2}{x}\right)^{|\nu|}. \tag{B.5}$$

For the order $\nu = 0$,

$$K_0(x) \sim \ln\frac{2}{x} - \gamma, \tag{B.6}$$

where γ is Euler's constant.

Appendix B.4. Fourier transform of a power function

$$\frac{1}{\sqrt{2\pi}} \int_{-\infty}^{\infty} \frac{1}{(k^2+l^2)^{\nu+1/2}} \, \mathrm{e}^{\mathrm{i}ly} \, \mathrm{d}y = \frac{\sqrt{2}}{\Gamma\left(\nu+\frac{1}{2}\right)} \left|\frac{y}{2k}\right|^{\nu} K_\nu(k|y|), \tag{B.7}$$

where ν is a real number that satisfies $\nu > -\frac{1}{2}$.

References

[1] Pierrehumbert R T, Held I M and Swanson K L 1994 *Chaos, Solitons Fractals* **4** 1111
[2] Held I M, Pierrehumbert R T, Garner S T and Swanson K L 1995 *J. Fluid Mech.* **282** 1
[3] Ohkitani K and Yamada M 1997 *Phys. Fluids* **9** 876
[4] Juckes M 1994 *J. Atmos. Sci.* **51** 2756
[5] Lapeyre G, Klein P and Hua B L 2006. *J. Phys. Oceanogr.* **36** 1577
[6] Yanase S and Yamada M 1984 *J. Phys. Soc. Jpn.* **53** 2513
[7] Larichev V D and McWilliams J C 1991 *Phys. Fluids* A **3** 938
[8] Watanabe T, Fujisaka H and Iwayama T 1997 *Phys. Rev.* E **55** 5575
[9] Watanabe T, Iwayama T and Fujisaka H 1998 *Phys. Rev.* E **57** 1636
[10] Iwayama T, Watanabe T and Shepherd T G 2001 *J. Phys. Soc. Jpn.* **70** 376
[11] Iwayama T, Shepherd T G and Watanabe T 2002 *J. Fluid Mech.* **456** 183
[12] Smith K S, Boccaletti G, Henning C C, Marinov I, Tam C Y, Held I M and Vallis G K 2002 *J. Fluid Mech.* **469** 13
[13] Schorghofer N 2000 *Phys. Rev.* E **61** 6572
[14] Watanabe T and Iwayama T 2004 *J. Phys. Soc. Jpn.* **73** 3319
[15] Tran C V 2004 *Physica* D**191** 137
[16] Watanabe T and Iwayama T 2007 *Phys. Rev.* E **76** 046303
[17] Gkioulekas E and Tung K K 2007 *J. Fluid Mech.* **576** 173
[18] Sukhatme J and Smith L M 2009 *Phys. Fluids* **21** 056603
[19] Tran C V, Dritschel D G and Scott R K 2010 *Phys. Rev.* E **81** 016301
[20] Iwayama T and Watanabe T 2010 *Phys. Rev.* E **82** 036307
[21] Ohkitani K 2012 *Phys. Fluids* **24** 095101
[22] Rayleigh L 1880 *Proc. London Math. Soc.* **11** 57
[23] Vallis G K 2006 *Atmospheric and Oceanic Fluid Dynamics* (Cambridge: Cambridge University Press)
[24] Press W H, Teukolsky S A, Vetterling W T and Flannery B P 1992 *Numerical Recipes in Fortran 77, the 2nd Ed., The Art of Scientific Computing* (Cambridge: Cambridge University Press)

[25] Whittaker E T and Watson G N 1927 *A Course of Modern Analysis* 4th Ed. (Cambridge: Cambridge University Press)
[26] Spiegel M R 1962 *Advanced Calculus* (New York: McGraw-Hill Book Company)
[27] Batchelor G K 1967 *An Introduction to Fluid Dynamics.* (Cambridge: Cambridge University Press)
[28] McIntyre M E and Shepherd T G 1987 *J. Fluid Mech.* **181** 527
[29] Watson G N 1944 *A Treatise on the Theory of Bessel Functions* 2nd Ed. (Cambridge: Cambridge University Press)